Biosensors and Bioelectronics 90 (2017) 53–60

Contents lists available at ScienceDirect

Biosensors and Bioelectronics

journal homepage: www.elsevier.com/locate/bios

Toxicity evaluation of e-juice and its soluble aerosols generated by electronic cigarettes using recombinant bioluminescent bacteria responsive to specific cellular damages

Shiv Bharadwaj[a], Robert J. Mitchell[b], Anjum Qureshi[a], Javed H. Niazi[a,*]

[a] Sabanci University Nanotechnology Research and Application Center, Orta Mahalle 34956, Tuzla, Istanbul, Turkey
[b] School of Life Sciences, Ulsan National Institute of Science and Technology, Ulsan 689-798, Republic of Korea

ARTICLE INFO

Keywords:
E-cigarette
E-juice
Toxicity
lux
Bioluminescence
Biosensor

ABSTRACT

Electronic-cigarettes (e-cigarette) are widely used as an alternative to traditional cigarettes but their safety is not well established. Herein, we demonstrate and validate an analytical method to discriminate the deleterious effects of e-cigarette refills (e-juice) and soluble e-juice aerosol (SEA) by employing stress-specific bioluminescent recombinant bacterial cells (RBCs) as whole-cell biosensors. These RBCs carry *luxCDABE*-operon tightly controlled by promoters that specifically induced to DNA damage (*recA*), superoxide radicals (*sodA*), heavy metals (*copA*) and membrane damage (*oprF*). The responses of the RBCs following exposure to various concentrations of e-juice/SEA was recorded in real-time that showed dose-dependent stress specific-responses against both the e-juice and vaporized e-juice aerosols produced by the e-cigarette. We also established that high doses of e-juice (4-folds diluted) lead to cell death by repressing the cellular machinery responsible for repairing DNA-damage, superoxide toxicity, ion homeostasis and membrane damage. SEA also caused the cellular damages but the cells showed enhanced bioluminescence expression without significant growth inhibition, indicating that the cells activated their global defense system to repair these damages. DNA fragmentation assay also revealed the disintegration of total cellular DNA at sub-toxic doses of e-juice. Despite their state of matter, the e-juice and its aerosols induce cytotoxicity and alter normal cellular functions, respectively that raises concerns on use of e-cigarettes as alternative to traditional cigarette. The ability of RBCs in detecting both harmful effects and toxicity mechanisms provided a fundamental understanding of biological response to e-juice and aerosols.

1. Introduction

The electronic cigarettes (e-cigarettes) are powered by battery-devices which uses the generated heat energy to transform the e-juice into the vapours that mimic the ordinary hand-to-mouth sensory experience of smoking to the user. The e-juice is a solution of nicotine in a mixture of glycerin, polyethylene or polypropylene glycol and flavoring additives (Brandon et al., 2015). The e-cigarettes are believed to be comparatively less harmful as well as an alternative to conventional smoking (Harrell et al., 2015). Therefore, e-cigarettes are progressively gaining popularity and prevalence in delivering vaporized nicotine (Allen et al., 2016). Howover, recent studies documented the toxic effects of e-juice on the human embryonic stem cells, human pulmonary fibroblasts cells and mouse neural stem cells (Bahl et al., 2012; Lerner et al., 2015). Moreover, the e-cigarette aerosols or e-vapours were also documented to be toxic to primary human bronchial epithelial cells (Scheffler et al., 2015) and human gingival fibroblasts (Sancilio et al., 2016) upon direct exposure. It is imperative to develop new in vitro techniques for rapid screening of cytotoxicity or genotoxic hazards of e-juice and its e-vapours, especially when new brands of e-cigarettes being progressively introduced into the market (Chu et al., 2015). The cartridges used to refill the e-cigarette have been detected with contaminants, such as diethylene glycol, heavy metals, silicate particles, and potential carcinogens, such as nitrosamines (Cheng, 2014; Orellana-Barrios et al., 2015; Williams and Talbot, 2011). Additionally, nicotine, also the main ingredient of e-cigarette known to produce reactive oxygen species (ROS) that trigger antioxidant imbalance and ROS-induced oxidative DNA damage in rat cells (Muthukumaran et al., 2008). Likewise, e-juice aerosols generated after heating in e-cigarette also contributes to ROS generation in cells (Lerner et al., 2015; Scheffler et al., 2015). Oxidative DNA damages by ROS, such as superoxide anion radicals ($^{\bullet}O_2^-$), hydrogen peroxide

* Corresponding author.
E-mail address: javed@sabanciuniv.edu (J.H. Niazi).

http://dx.doi.org/10.1016/j.bios.2016.11.026
Received 3 October 2016; Received in revised form 7 November 2016; Accepted 8 November 2016
Available online 12 November 2016
0956-5663/

(H_2O_2) and hydroxyl radicals ($^{\bullet}OH$) induce mutations, breaks in DNA strands and lesions causing various diseases including cancer (D'Errico et al., 2008).

Considering the limited knowledge of health impacts of e-cigarettes, it is imperative to explore its potential impact on living cells. Recombinant Bacterial Cells (RBCs) can be used as living biosensors to rapidly evaluate and analyse the toxicity of e-juice/liquids and associated e-aerosols (e-vapours) at their sub-toxic concentrations. The RBCs harbour a reporter operon which is strictly governed by the transcriptional regulating promoters specific to target chemical/agent that generate an output signal in the form of light or color. Such biological sensors provide a cost effective, rapid, easy and alternative means to assess specific toxicity modes of target chemicals, such as those present in the e-juice. This type of biosensors has been used for long in various biosensing experiments (He et al., 2016). For instance, *recA* promoter is transcriptionally fused with the green fluorescence protein gene (GFP) to screen the bacterial DNA inhibitors via the SOS response (Fan et al., 2014), and *sodA* regulating GFP is used in bioassays for drug screening (Elad et al., 2015).

In this study, we have investigated the toxicity of e-juice and its aerosols at sub-toxic doses by employing four distinct stress-specific RBCs as biosensors. These bacterial biosensors emit light by expressing stress-specific promoters upstream of *Photorhabdus luminescens luxCDABE* genes present on a plasmid in recombinant *E. coli* against cellular damages, such as DNA damage, oxidative stress by superoxide radical, heavy metals (copper) and membrane damage. The light emission responses against the chemical stimuli in RBCs is the signature of toxicity in cells and the specific promoter provide information on type cellular damage. Here, sub-toxic stress concentration of chemicals present in e-juice and aerosols were determined. Our results demonstrated that the liquid and aerosol forms of e-juice had distinct impact on living cells. Direct cellular interaction with diluted e-liquids imposed growth inhibition and repression of genes responsible for cellular repair mechanism and heavy metal homeostasis. Higher e-liquid concentrations could lead to total cellular DNA-fragmentation. However, e-juice in aerosol forms showed no growth inhibition but induced the genes of cellular repair mechanisms in an effort to mitigate cellular stress. Such an approach to accessing the toxicity of e-juice and e-vapours/aerosols could provide first information on overall cellular responses that may be useful for further studies on their toxicity using human cells.

2. Materials and methods

2.1. Plasmids, bacterial strains and chemicals

The plasmids and stress-inducible bioluminescent recombinant bacterial cells used in this study are listed in Table S1. All strains were grown in either synthetic-M9 or LB-broth medium (Difco MI, USA) depending upon the specified experimental conditions. The commercial e-juice (NJOY) was purchased from a local vendor that according to the manufacturer, contained glycerin, propylene glycol, nicotine (10 mg/mL) and other flavoring chemicals. All other reagents used were of analytical grade. The RBCs were designed to specifically respond to DNA damage (*E. coli*-RecA), oxidative toxicity (*E. coli*-SodA), heavy metal (*E. coli*-CopA) and membrane damage (*E. coli*-DMO1). Fig. 1a-e shows map of plasmid carried by each RBC that were utilized to screen the harmful effects of e-juice and SEA.

2.2. Determination of effective concentration at half maximum toxicity (EC50)

The stress-specific bioluminescent bacteria and control cells were treated with a series of e-juice dilutions in M9-medium and EC50 was determined as described in Supporting information (SI) section.

2.3. Preparation of bubble-solubilized e-juice aerosols

The engineered design and used materials in the e-cigarettes could also affect the chemical characteristics and potential toxicity of released e-vapours/aerosols from the e-cigarettes (Brown and Cheng, 2014; Kosmider et al., 2014). Therefore, in this study we utilized a concentration chamber equipped with an inlet and outlet to collect the released e-cigarette aerosols (e-vape) by bubble-solubilizing in synthetic M9-medium (Fig. 1a-b). About, 1.8 mL of concentrated e-juice refill (10 mg/mL of nicotine+other ingredients) was loaded in the e-cigarette device and puffed through the atomizer into 22.5 mL of synthetic M9-medium with the help of an inlet tube connected to the mouthpiece of the device and a vacuum suction at the outlet of the concentration chamber. Finally, the bubble-solubilized e-cigarette aerosols (SEA) (0.8 mg/mL with respect to nicotine content) in M9-medium was further diluted to various dilutions below EC50 levels and used for toxicity screening with RBCs.

2.4. UV–vis spectra, cell growth and bioluminescence assays

The UV–vis spectra of e-juice in liquid form and SEA were recorded between 200 and 350 nm using NanoDrop 2000 UV–Vis spectrophotometer. The sub-toxic to lethal effects of e-juice and SEA (diluted 4–256-folds) were exposed to four stress-specific bioluminescent recombinant *E. coli* cells shown in Table S1. Each strain contained a plasmid carrying a fusion of promoter and reporter *luxCDABE* from *Photorhabdus luminescens*, where the promoter specifically responds to toxicity, such as genotoxicity (*recA*), heavy metals (*copA*), superoxide stress (*sodA*) and membrane integrity (*oprF*) upstream of the *luxCDABE* gene cassette (Table SI). The recombinant bacterial strains carrying *recA::luxCDABE*, *sodA::luxCDABE, copA::luxCDABE* and *oprF::luxCDABE* were pre-grown in 5 mL of M9–broth media (Difco MI, USA) for 14 h at 37 °C with constant shaking (120 rpm). The cells were harvested by centrifugation at 5000 rpm for 10 min and washed thrice with PBS (pH 7.6). These cells were then re-suspended across the 96-well white plates with transparent bottom (BRANDplates®) in a way that allow different concentrations of e-juice/SEA present in 100 µL synthetic M9-media with initial absorbance of 0.22 at 600 nm or ~1.8×10^8 cells/mL for bioluminescence assays. Besides, culture media containing no e-juice/SEA were also inoculated under identical conditions and used as standard controls for comparison. The white 96-well plates with transparent bottom allowed simultaneous measurement of both bioluminescence and absorption at 600 nm in a Synergy HTX-multimode microplate reader (Biotek) equipped with a photomultiplier tube (PMT) to collect whole photons from recombinant strains and the microplate reader computed the generated signal into relative arbitrary light units (RLU, bioluminescence). Both absorbance and bioluminescence of the RBCs were recorded at every 10 min intervals for 8 h. Other assay controls such as those interfering in the media and e-juice were taken into consideration and used as appropriate blanks for normalization. Moreover, net bioluminescence induction caused by the model chemicals in RLU was divided by the OD600 to correct for variations in cell density as reported previously (Elad et al., 2015). All the bioluminescence raw data was subjected to normalization and histogram and clustering was generated using clustergram tool in Matlab software.

All assays were conducted in replicates (n=3) and normalized with appropriate assay controls and the % relative standard deviations (% RSD) was calculated to be less than 11%.

2.5. Cell viability and e-juice mediated DNA fragmentation assay (alkaline gel electrophoresis)

Cell viability was performed using 1.8×10^8 cells/mL treated with maximum (1:4 dilution or 2.5 mg/mL) and least minimum (1:64 dilution or 0.156 mg/mL) doses of e-juice amended in PBS solution.

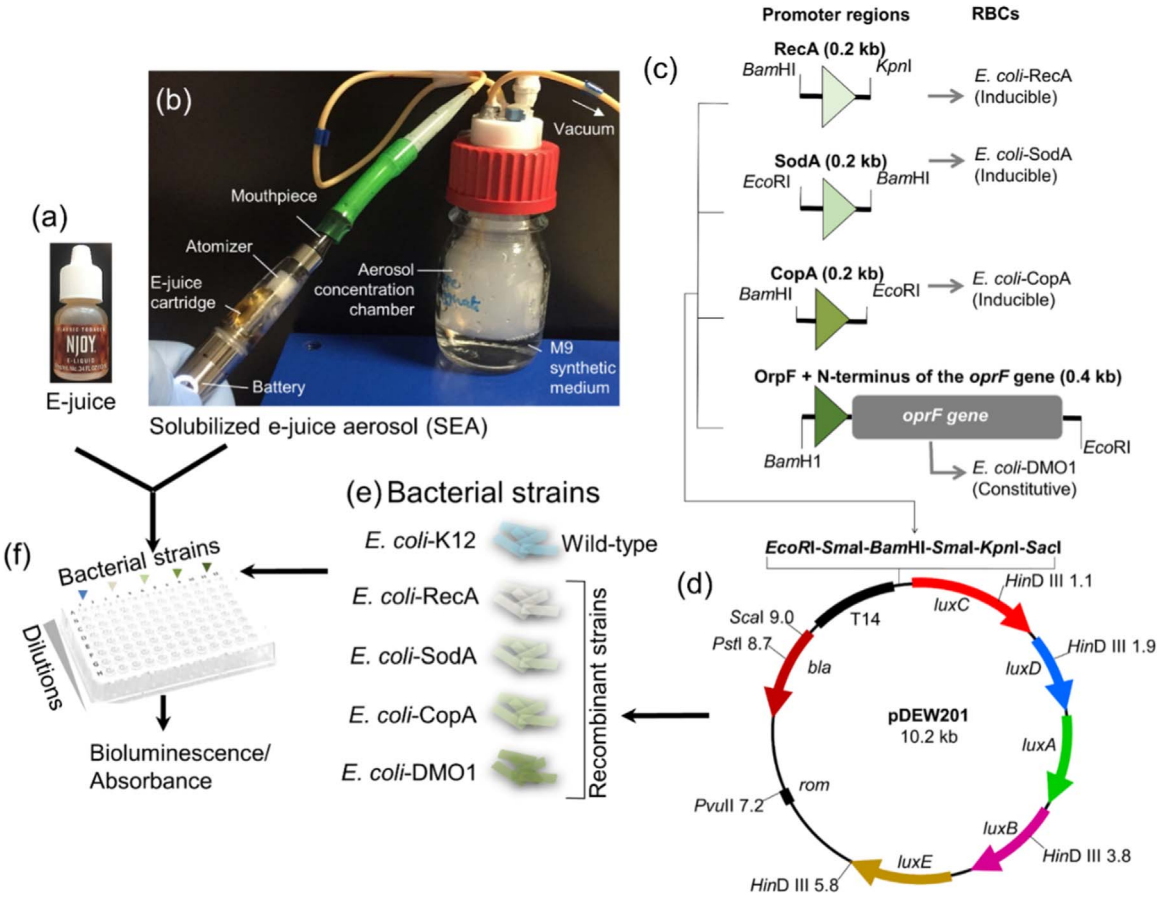

Fig. 1. (a) Commercial concentrated e-juice/liquid and (b) real image showing a charged e-cigarette device whose mouthpiece connected to an inlet tube immersed in a synthetic M9-medium in a concentration chamber for sampling SEA. The outlet tube from the chamber opened to empty space in the chamber which is connected to vacuum. The vacuum generates suction that enables e-vapours to bubble-dissolve in the medium. (c) *E. coli* promoter regions that regulate *recA*, *sodA*, *copA* and *oprF* genes are placed upstream of *luxCDABE* operon in pDEW201 with ampicillin resistance (*bla*). (d) A map of promoter-less pDEW201 base plasmid (Lee et al., 2013). (e) The recombinant bacterial cells carrying specific promoter-*luxCDABE* fusion and (f) e-juice and SEA were serially diluted in a 96-well microtiter plate and real-time absorbance and bioluminescence were recorded.

Details of cell-viability and DNA fragmentation assays are described in SI section.

3. Results

3.1. UV–Vis spectra of e-juice and solubilized e-juice aerosols

UV–Vis spectra of the dilute e-juice in liquid form as well as bubble-dissolved SEA produced from the e-cigarette after puffed through the fresh synthetic M9-medium showed a total of five overlapping peaks (Fig. 2). Peaks at 254, 260 and 265 nm represent e-juice nicotine in M9-medium at pH 7.6 consistent to that previously reported (Clayton et al., 2013). The major peaks at 200–220 nm in both UV-spectra of e-juice and its SEA seem to have originated due to the additional chemical ingredients present in e-juice.

3.2. Response of RBCs to e-juice in liquid form

Wild-type and model biosensor cells, such as *E. coli*-K12 (wild-type, control), *E. coli*-RecA (*recA::luxCDABE*), *E. coli*-SodA (*sodA::luxCDABE*), *E. coli*-CopA (*copA::luxCDABE*) and *E. coli*-DMO1 (*oprF::luxCDABE*) responsive to DNA-damage, oxidative stress, heavy metal and membrane damage, respectively were treated with standard chemicals, such as mitomycin C (MMC), hydrogen peroxide (H_2O_2), copper sulfate ($CuSO_4$) and phenol, respectively and the results are shown in Fig. S1. All the strains were treated with varying e-juice concentrations and the results showed a dose-dependent inhibition in bioluminescence signals with EC50=0.71, 0.76, 0.66,

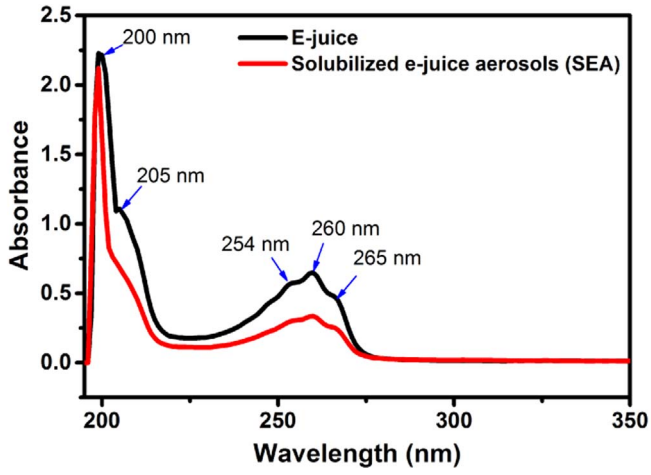

Fig. 2. The UV–Vis absorption spectra of e-juice and solubilized e-juice aerosols (SEA) in the synthetic-M9 media (pH 7.6) showing overlapping peaks of chemical ingredients.

0.25, 0.54 mg/mL nicotine in e-juice, respectively (Fig. S2). Maximum growth inhibition occurred at 1.25 mg/mL (8-folds diluted) with e-juice in liquid form, and this trend was reflected on their bioluminescence responses (Fig. 3a-d). Significant increase in bioluminescence was observed after 60 min interval by all tested biosensor cells, indicating remarkable stress sensitivity against e-juice. On further incubation beyond 60 min, except with 2.5 (4-folds diluted) and 1.25 (8-folds diluted) mg/mL, all the biosensor cells exhibited incremental

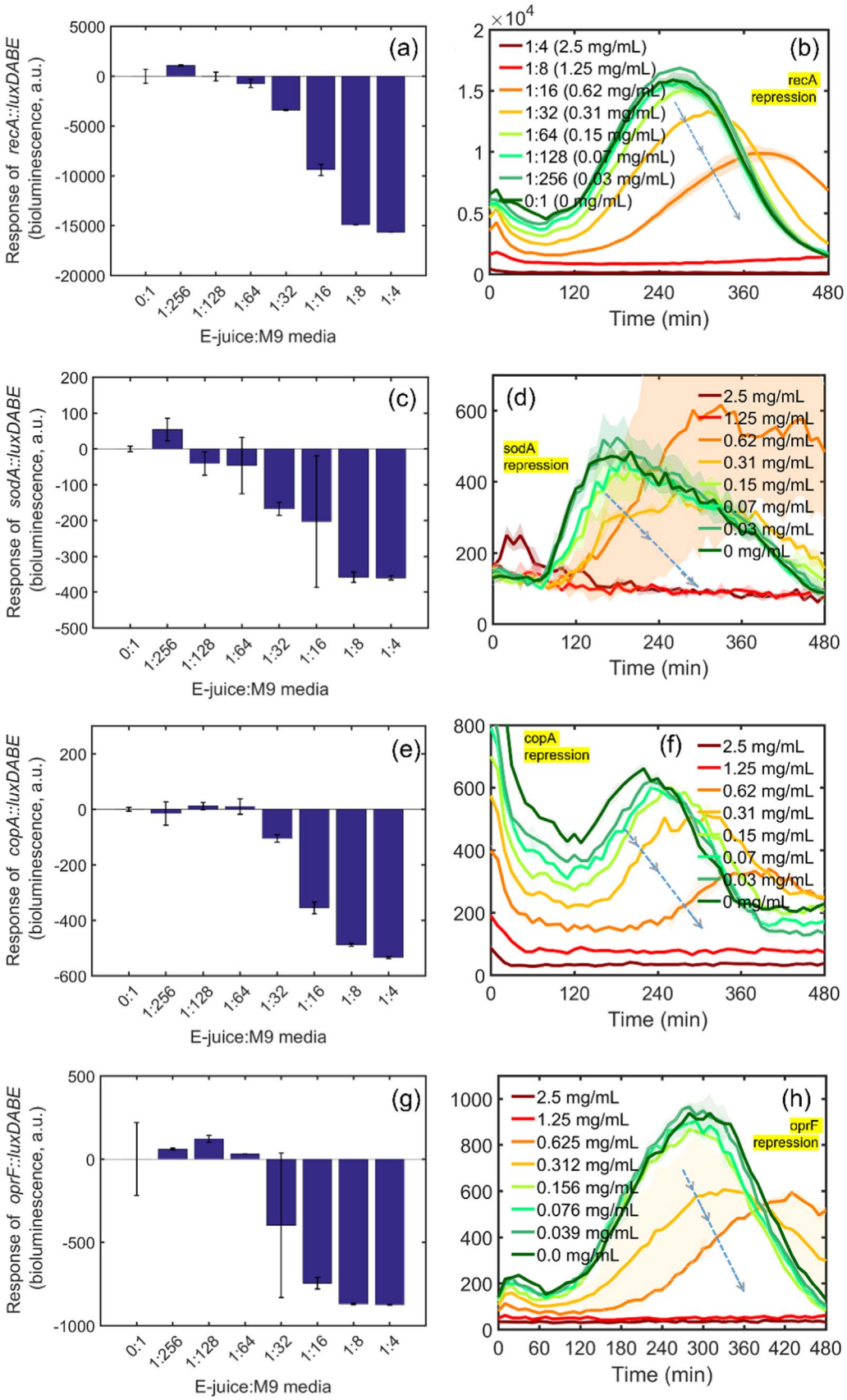

Fig. 3. Bioluminescence signals (arbitrary light units, a.u.) generated by recombinant *E. coli* whole-cell biosensors responsive to specific toxicity: (a-b) DNA damage (*recA::luxCDABE*), (c-d) superoxide radicals (*sodA::luxCDABE*), (e-f) heavy metals (*copA::luxCDABE*) and (g-h) membrane damage (*oprF::luxCDABE*) after the treatment with e-juice (e-liquid) directly mixed in M9-medium at a series of dilutions shown in figure legend of (b). The concentrations (mg/mL) in the legend are representatives of the actual nicotine levels present in the diluted samples. The left column showing bar plots of relative bioluminescence responses from respective biosensor strains carrying specific promotor-lux fusion (*y*-axis titles) at a maximum response time (within 180–270 min). The right column shows time-course bioluminescence responses from 0 to 480 min. The standard errors are shown in shaded areas with matching colors.

bioluminescence profiles with e-juice dilutions (e-juice: M9=1:16 to 1:256 times dilutions). Furthermore, induction levels in bioluminescence (high to low) with respect to e-juice dilutions (0.625–0.039 mg/mL) after 60 min followed the trend: *E.coli*-RecA > *E.coli*-CopA > *E.coli*-DMO1 > *E.coli*-SodA (Fig. 3a-d). This trend was also reflected on the growth of RBCs where growth inhibition is clearly evident with high e-juice concentrations mixed in M9-medium (Fig. S3a-d, panel I). These results suggest that the toxicity of e-juice was mainly caused by the inhibition or blocking of DNA repair mechanism leading to cell growth inhibition, which is consistent to previously reported studies (Bahl et al., 2012). Interestingly, *E.coli*-RecA and *E.coli*-SodA tend to induce with a threshold concentration of 0.039 mg/mL (1:256 diluted), which indicates the potential single-stranded DNA damage and chronic production of superoxide ($O^{2\bullet-}$) radicals, respectively. However, *E.coli*-CopA strain responsible for inducing to heavy metal toxicity showed inhibition of bioluminescence response suggesting the possibility that the selected sub-toxic doses of e-juice may disrupt the cells' ability to balance metal ion homeostasis (e.g., copper ions). Therefore, e-juice/liquid likely to cause the inhibition or damage to *copA* gene cassette essential for heavy metal ion pumps. Contrastingly, the bacterial biosensor *E. coli*-DMO1 which carries a membrane damage responsive *oprF::luxCDABE* fusion was sensitive to even very low e-juice concentrations (1:128-256 diluted e-juice or 0.15–0.03 mg/mL nicotine) suggesting that e-juice can cause detrimental changes in the outer cell membrane (Fig. 3d).

We observed that the maximum RBCs' responses to the liquid form of e-juice tend to decline dose-dependently, but with maximum response time shifts (MRT) observed from 180 to 240 min after the exposure. The MRT seem to be associated with the reduction in number of cells due to growth inhibition. Therefore, cell viability tests were performed by viable cell counts after treating cells with least minimum inhibitory (1:64 dilution or 0.156 mg/mL) and maximum inhibitory (1:4 dilution or 2.5 mg/mL) doses of e-juice amended in PBS and plated on LB-agar. Fig. S4 shows the viable cells obtained after the treatment of bacterial cells showing 87–90% and 42–51% inhibition, respectively compared with the controls (Table S2 and Fig. S4). These results are consistent with those of bioluminescence signals (repressed the expression of *recA*, *sodA*, *copA* and *oprF* promoters) from cells treated with diluted e-juice in M9 (Fig. 3a-d) and growth inhibition (Fig. S3a-d, panel I).

3.3. Response of RBCs to solubilized e-juice aerosols (SEA)

SEA was first prepared by bubble-dissolving liquid e-juice (1.8 mL as per the volume for one e-cigarette refill) in M9-medium as described in experimental methods. Biosensor cells were exposed to a series of various SEA dilutions (4–256 folds) in M9-medium. Fig. 4a-d show bioluminescence responses that consistently induced with concentrated SEA (SEA: M9=1:4 to 1:32) except *E. coli*-SodA which showed highly dynamic bioluminescence induction throughout the course of SEA exposure (Fig. 4b). Therefore, the prepared dilutions of SEA hold the potential to induce superoxide ($O^{2\bullet-}$) radical formation, as evidenced by the *E. coli*-SodA response, unlike the cells treated with e-juice responded only to the very low doses (Figs. 3a-d and 4a-d). *E. coli*-CopA and *E. coli*-DMO1 cells were highly sensitive to SEA and exhibited maximum induction levels that can be directly linked to cellular mitigation against the heavy metal toxicity and membrane/osmotic stress (Fig. 4c-d). *E. coli*-CopA responses, however, was distinct which spontaneously emitted light soon after the SEA exposure, indicating the sensitivity of designed biosensor towards the heavy metal contamination in the e-juice aerosols. Additionally, *E. coli*-CopA also represents the bioluminescence for lower dilutions unlike those cells treated with e-juice required maximum concentrations, suggesting the heavy metal specific stress-response decreases with the dilution of heavy metal (copper) in the dissolved aerosols (Figs. 3c and 4c). The above results revealed the dose-dependent genotoxicity and cytotoxicity of the dissolved aerosols at such lower concentrations, again provides an insight into the potential hazards of e-cigarette aerosols, compared to e-juice alone in liquid form. Remarkably, no reduction in bioluminescence was observed at higher dilutions of SEA which shows its non-toxicity to cells. This result was further supported by the growth studies where cells treated with different dilutions of SEA showed no significant difference in comparison to their respective controls (Fig. S3, panel II, a-d). However, this observation provides the evidence that the sensitivity and ability of engineered cells to distinguish or detect the potential toxicity of e-juice in both liquid and aerosols forms at sub-toxic levels.

3.4. Cellular DNA fragmentation analysis

We hypothesized that the different concentrations of e-juice potentially cause damage to the total cellular DNA in the model bacterial biosensor cells and thus showed inhibition of light emission at high concentrations. This hypothesis was tested with the wild type *E. coli*-K12 and four genetically modified bacterial cells that were nursed with the 2.5 and 0.156 mg/mL as maximum and least minimum inhibitory e-juice concentrations, respectively for 2 h in PBS. Following the treatment, the whole bacterial cells were subjected to alkaline gel electrophoresis for determining fragmented DNA due to the damage as described in experimental methods. Fig. 5 shows an alkaline gel showing two types of DNA bands; (i) the intense bands of supercoiled genomic DNA tangled or trapped in cells and remain immobilized in the wells of agarose gel, (ii) fragmented genomic DNA appeared as smears after the cells present the damaged genomic DNA from the cells in gel-wells. Cells treated with maximum dose (2.5 mg/mL or 1:4-folds) of diluted e-juice showed no entrapment of genomic DNA in the wells because the fragmented DNA running down in the gel was clearly visible (Fig. 5). The minimum dose (0.156 mg/mL or 1:64-folds) of dilute e-juice however showed partial DNA fragmentation with less DNA intensity retained in the wells. These results demonstrated that high-doses of e-juice in liquid forms induced remarkable DNA breaks compared to that observed with low-doses or controls.

4. Discussion

E-cigarettes have gained popularity because of their ability to deliver vaporized nicotine and passive smoking. This has led to speculation about safety of e-cigarettes due to lack of sufficient evidence on their harmful effects. In this regard, designing and validation of laboratory models can be used to determine the side effects or consequences of e-cigarettes in the biological system. To address this problem, we have used stress-specific promoters regulating the *lux* gene cassette to produce the toxicological evidence against e-juice in model RBCs as biosensors. Our results revealed that nicotine amended e-juice inhibits the bioluminescence emission in all bacterial biosensors at high concentration, while significant emission can also be seen at lower concentrations (Fig. 6a). Contrastingly, the bioluminescence profiles from the recombinants strains exposed to the different concentrations of SEA showed an opposite effect, where the bioluminescence signal increased dose-dependently (Fig. 6b). The heatmaps in Fig. 6a-b illustrate an overall response of e-juice in two different physical states (liquid/aerosol) that significantly affected the biological system. The SEA did not affect the cellular growth but strongly induced genes engaged in mitigating the stress responses (Figs. S3a-d, panel II; 3a-d; 4a-d).

It is well documented that nicotine can induce the production of ROS which further results into significant decrease in the endogenous antioxidant status of the cell (Muthukumaran et al., 2008). Additionally, Arany et el. reported the inhibition of superoxide dismutase, catalase, glutathione peroxidase activities and reduced glutathione in the cell occurred due to the chronic exposure of nicotine (Arany et al., 2013). Such effects implicate oxidative stress in cells

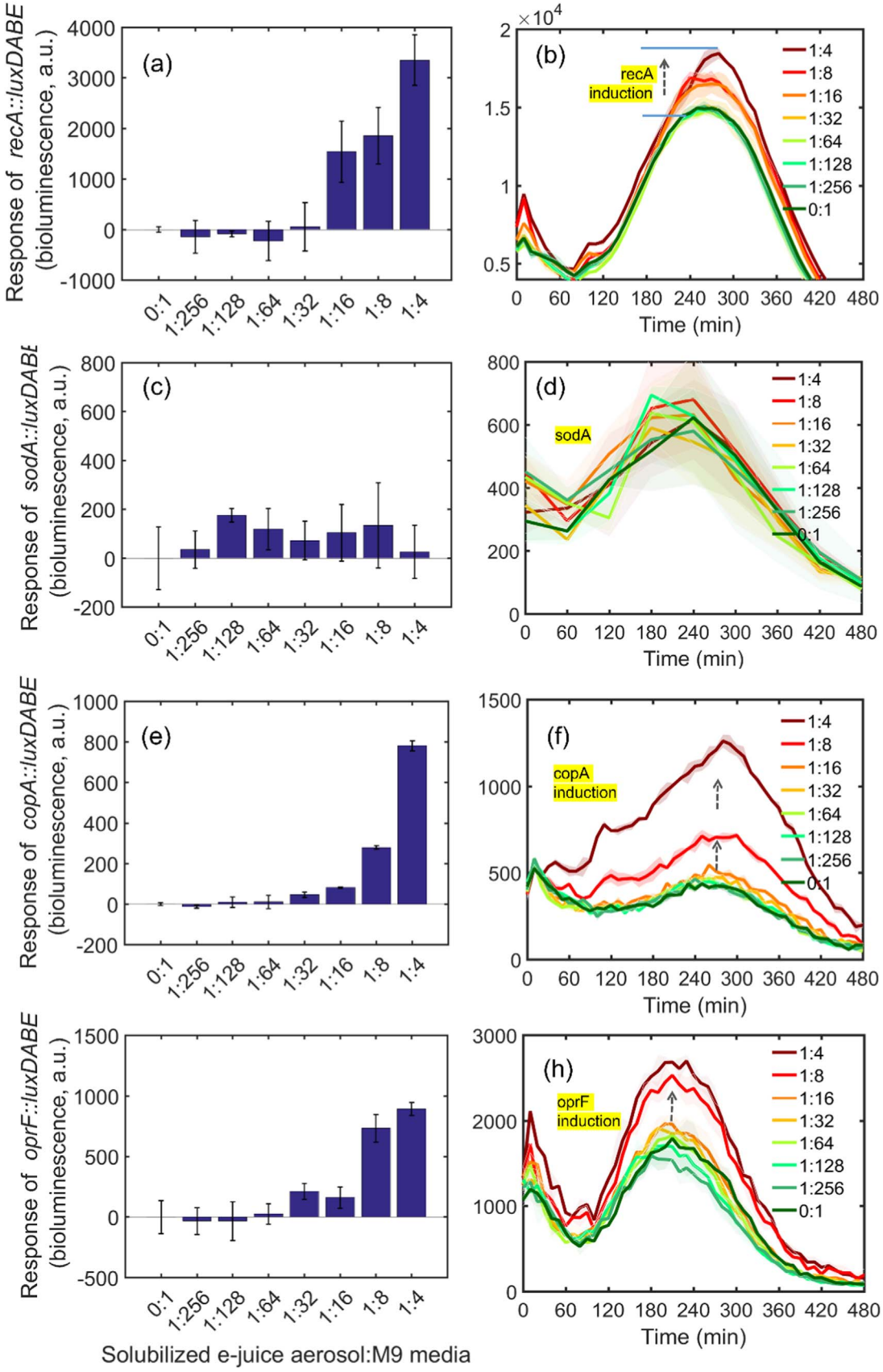

Fig. 4. Bioluminescence signal generated form cells exposed to e-juice vapours (aerosols). The vapours were first bubble-dissolved from 1.8 mL e-liquid in 22.5 mL of M9-medium (equivalent to 1.25 mg/mL nicotine levels). The solubilized e-juice aerosol solution was subjected to treatment with four recombinant *E. coli* whole-cell biosensors responsive to; (a-b) DNA damage (*recA::luxCDABE*), (c-d) superoxide radicals (*sodA::luxCDABE*), (e-f) heavy metals (*copA::luxCDABE*) and (g-h) membrane damage (*oprF::luxCDABE*) at a series of dilutions shown in figure legends. The bar plots on left column show relative bioluminescence responses extracted at maximum response times (180–270 min). The right column shows the time-course bioluminescence profiles during 0–480 min and the standard errors are shown in shaded area with matching colors.

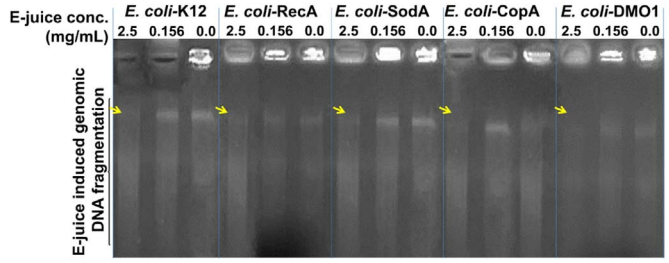

Fig. 5. Five *E. coli* strains (1.8×10^8 cells/mL) were treated with maximum (2.5 mg/mL or 1:4 fold) and minimum (0.156 mg/mL or 1:64 fold) inhibitory doses of e-juice liquid in PBS solution were loaded along with untreated cells on an alkaline agarose gel and electrophoresed in alkaline buffer at 10 V for 14 h. The gel was post-stained with ethidium bromide after neutralization and the picture was taken under the UV-light. The fragmented DNA due to high doses of e-juice (yellow arrow highlighted) can be seen as smears running down the gel. The non-fragmented DNA tangled with cells was seen trapped in control-wells and low-dose treated cells.

leading to activation of multiple intracellular signaling pathways and cell death (Ogura and Shimosawa, 2014). We speculate that the toxic levels of e-juice can damage DNA or inhibit growth through arresting normal cellular functions, such as ROS defense system. Meanwhile, at low concentrations, the cells may develop resistance easily in comparison to high concentrations and hence elicit the light emission, except for *E.coli*-CopA. This assumption was found true when the biosensor cells were exposed to 2.5 mg/mL of nicotine in e-juice that showed significant growth loss as evidenced by reduced number of CFU against 0.156 mg/mL concentration (Figs. S2, S4 and Table S2).

Recently, it is documented that the oxidative stress caused by nicotine is also responsible for inducing DNA damage in epithelial cells (Ginzkey et al., 2012). Therefore, it was imperative to test the DNA damage in cells treated with e-juice that had shown significant reduction in growth. Our results revealed that high-doses of e-juice likely to induce cellular DNA fragmentation at least in bacterial models (Fig. 6). It remains to be seen if this is also true in human cells. This result provides early evidence that cell inhibition/death can be possible at higher doses that seem to occur due to the chemical ingredients/flavourings present in the e-juice. Furthermore, chemicals known to be harmful are present in e-cigarette aerosol and their effect could also depend on several variables, such as the solution used and the battery output voltage (Bahl et al., 2012; Kosmider et al., 2014). Also, the levels of toxic product may depend on the way the e-cigarette is used (Farsalinos et al., 2015).

The heated e-liquid emissions shown to contain the carcinogenic carbonyl compounds formaldehyde and acetaldehyde (Goniewicz et al., 2014; Jensen et al., 2015; Kosmider et al., 2014), ROS, heavy metals, and volatile organic compounds, such as toluene that will have detrimental effects on living cells (Goniewicz et al., 2014; Lerner et al., 2015; Williams and Talbot, 2011). In this study, we addressed these effects with bacterial biosensors that were treated against different dilutions of e-juice and SEA. Our results indicated that the impact of e-juice at least in bacterial model tend to diminish with dilutions of chemical ingredients present in e-juice (Figs. 3a-d, 4a-d and 6a-b). Moreover, the transformation of e-juice into e-vapours by heat produced more free radicals, which in turn increase the e-vapour toxicity (Sussan et al., 2015). Hence, *E. coli*-SodA treated with different dilutions of dissolved e-juice aerosols showed significant light emission when compared with control cells. The *E. coli*-RecA induced high bioluminescence emission only at the high doses of SEA probably because of its ability to oxidatively damage DNA with free $O^{2\bullet-}$, which decreased with dilution factor and hence, low bioluminescence emission from the cells (Fig. 4a). Furthermore, the recombinant *E. coli*-CopA showed high bioluminescence at high concentration indicates the presence of copper in the dissolved aerosols, which reduced in the media with the dilution. It is to be noted that the contamination of copper could occur by the oxidation of heating coil in e-cigarette device as it has been previously reported (Williams et al., 2013).

5. Conclusion

E-cigarettes deliver aerosol containing nicotine to users by heating e-liquid/juice. Typically, e-juice contains a mixture of glycerin, propylene glycol and various other flavoring chemicals. The potential adverse effects of a variety of flavoring chemical combinations used in e-juice

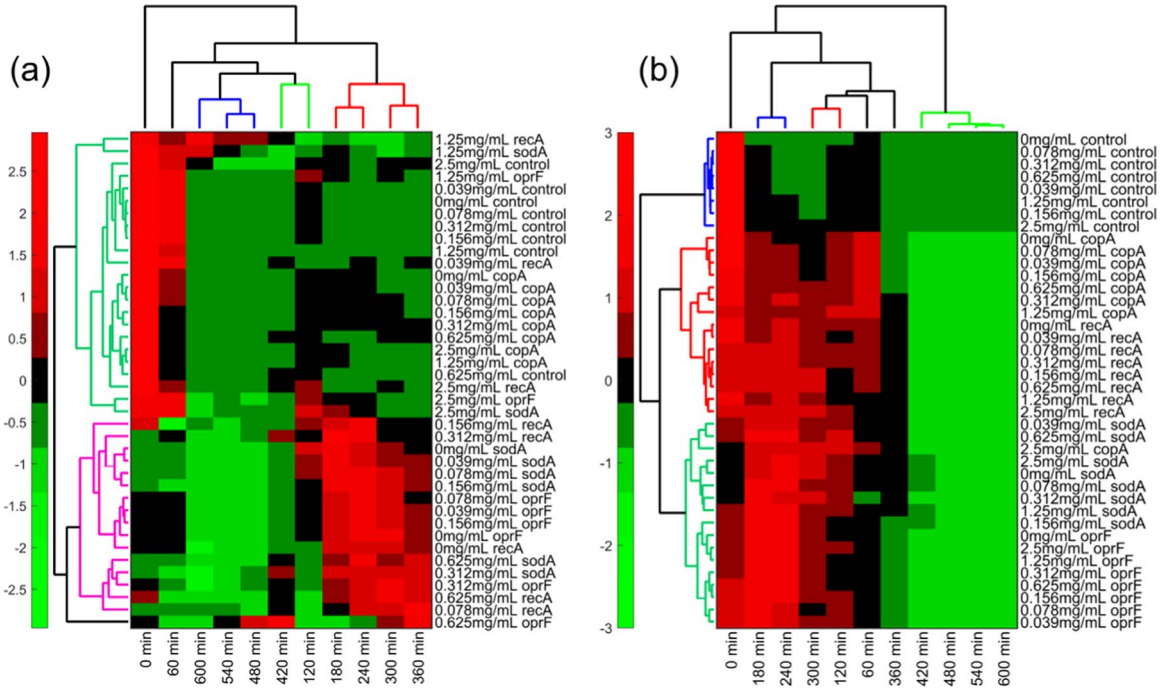

Fig. 6. Heatmaps and clustering of the bioluminescence response data measured at different time intervals as shown in *x*-axis against; (a) e-juice in liquid form mixed in M9-medium, and (b) Solubilized e-juice aerosol (SEA) in M9-medium. The colors red, black and green represents induction, unchanged or repressed bioluminescence responses from cells against different concentration indicated on *y*-axis along with strain identities, such as *recA* (*E. coli*-RecA), *sodA* (*E. coli*-SodA), *copA* (*E. coli*-CopA) and *oprF* (*E. coli*-DMO1).

remains largely unexplored. Considering the fastest-growing e-cigarette industry, a rapid and versatile screening method is needed to assess their toxicant exposure and potential risk to ensure safety. Herein, we used four stress-specific recombinant bioluminescent *E. coli* cells explicitly respond to single stranded DNA breaks (*recA::luxCDABE*), reactive oxygen species (*sodA::luxCDABE*), heavy metal such as copper (*copA:: luxCDABE*) and cell membrane damage (*oprF::luxCDABE*). These RBCs provided real-time biological responses to liquid e-juice and e-cigarette generated SEA in limited mineral medium with glucose as the only carbon and energy source. This allowed bioluminescent RBCs to sensitively emit specific bioluminescence light to the e-juice/SEA toxicants. As a result, bioluminescent RBCs provided the strong evidences that revealed sub-toxic doses of e-juice and SEA induce cytotoxicity. We found that the liquid form of e-juice suppressed the cellular ability to repair DNA damage, ion homeostasis, oxidative toxicity and membrane disruption caused by the e-juice. SEA also exhibited toxicity but the level of this toxicity was not as lethal as it was with the liquid e-juice. Therefore, bioluminescent RBCs acquired the ability to adapt against the toxicants in SEA by recruiting inducible cellular repair mechanisms, thus enabling cells to preserve their normal growth rate and reverse the SEA toxicity.

RBCs served as whole-cell living biosensors to simultaneously detect both cytotoxicity and intrinsic toxicity mechanisms taking place against e-juice and SEA. Biological responses from these RBCs can be used as surrogate responses relevant to human health risk assessments. However, there is an intrinsic limitation in using multiple RBCs responsive to distinct type of toxicities and thus differential bioluminescence patterns, respectively. Therefore, choice of appropriate cell population size for each RBC type relevant to dose and intensity of bioluminescence light emission is imperative. Further, real-time toxicity monitoring for continuous screening with solubilized e-juice aerosols from various other e-juice flavoring combinations is required. Our future directions are toward developing a series of other new RBCs, each specific to a different type of cytotoxicity that potentially contribute to a comprehensive understanding on the major cellular responses against e-juice and SEA. For this, a multi-reactor setting may be needed that may be equipped to continuously and simultaneously detect long-term cytotoxicity.

Acknowledgements

This work was supported by the Scientific and Technological Research Council of Turkey (TUBITAK), Project Grant no. 114E101. We thank Hansol Im for helping with pCopA plasmid construction.

Appendix A. Supporting information

Supplementary data associated with this article can be found in the online version at doi:10.1016/j.bios.2016.11.026.

References

Allen, J.G., Flanigan, S.S., LeBlanc, M., Vallarino, J., MacNaughton, P., Stewart, J.H., Christiani, D.C., 2016. Environ. Health Perspect. 124 (6), 733–739.
Arany, I., Clark, J., Reed, D.K., Juncos, L.A., 2013. Nephrol. Dial. Transpl. 28 (6), 1417–1425.
Bahl, V., Lin, S., Xu, N., Davis, B., Wang, Y.H., Talbot, P., 2012. Reprod. Toxicol. 34 (4), 529–537.
Brandon, T.H., Goniewicz, M.L., Hanna, N.H., Hatsukami, D.K., Herbst, R.S., Hobin, J.A., Ostroff, J.S., Shields, P.G., Toll, B.A., Tyne, C.A., Viswanath, K., Warren, G.W., 2015. J. Clin. Oncol. 33 (8), 952.
Brown, C.J., Cheng, J.M., 2014. Tob. Control 23, 4–10.
Cheng, T.R., 2014. Tob. Control 23, 11–17.
Chu, K.H., Unger, J.B., Allem, J.P., Pattarroyo, M., Soto, D., Cruz, T.B., Yang, H.D., Jiang, L., Yang, C.C., 2015. PLoS One 10, 12.
Clayton, P.M., Vas, C.A., Bui, T.T., Drake, A.F., McAdam, K., 2013. Chirality 25 (5), 288–293.
D'Errico, M., Parlanti, E., Dogliotti, E., 2008. Mutat. Res. 659 (1–2), 4–14.
Elad, T., Seo, H.B., Belkin, S., Gu, M.B., 2015. Biosens. Bioelectron. 68, 699–704.
Fan, J., de Jonge, B.L.M., MacCormack, K., Sriram, S., McLaughlin, R.E., Plant, H., Preston, M., Fleming, P.R., Albert, R., Foulk, M., Mills, S.D., 2014. Antimicrob. Agents Chemother. 58 (12), 7264–7272.
Farsalinos, K., Voudris, V., Poulas, K., 2015. Addiction 110 (11), 1862–1864.
Ginzkey, C., Stueber, T., Friehs, G., Koehler, C., Hackenberg, S., Richter, E., Hagen, R., Kleinsasser, N.H., 2012. Toxicol. Lett. 208 (1), 23–29.
Goniewicz, M.L., Knysak, J., Gawron, M., Kosmider, L., Sobczak, A., Kurek, J., Prokopowicz, A., Jablonska-Czapla, M., Rosik-Dulewska, C., Havel, C., Jacob, P., Benowitz, N., 2014. Tob. Control 23 (2), 133–139.
Harrell, P.T., Marquinez, N.S., Correa, J.B., Meltzer, L.R., Unrod, M., Sutton, S.K., Simmons, V.N., Brandon, T.H., 2015. Nicotine Tob. Res. 17 (2), 193–200.
He, W., Yuan, S., Zhong, W.H., Siddikee, M.A., Dai, C.C., 2016. Appl. Microbiol Biotechnol. 100 (3), 1109–1119.
Jensen, R.P., Luo, W., Pankow, J.F., Strongin, R.M., Peyton, D.H., 2015. N. Engl. J. Med. 372 (4), 392–394.
Kosmider, L., Sobczak, A., Fik, M., Knysak, J., Zaciera, M., Kurek, J., Goniewicz, M.L., 2014. Nicotine Tob. Res. 16 (10), 1319–1326.
Lee, S., Amasia, M., Madou, M., Mitchell, R.J., 2013. Biosens. Bioelectron. 46, 175–182.
Lerner, C.A., Sundar, I.K., Yao, H.W., Gerloff, J., Ossip, D.J., McIntosh, S., Robinson, R., Rahman, I., 2015. Plos One 10, 2.
Muthukumaran, S., Sudheer, A.R., Menon, V.P., Nalini, N., 2008. Toxicology 243 (1–2), 207–215.
Ogura, S., Shimosawa, T., 2014. Curr. Hypertens. Rep. 16, 8.
Orellana-Barrios, M.A., Payne, D., Mulkey, Z., Nugent, K., 2015. Am. J. Med 128 (7), 674–681.
Sancilio, S., Gallorini, M., Cataldi, A., di Giacomo, V., 2016. Clin. Oral Investig. 20 (3), 477–483.
Scheffler, S., Dieken, H., Krischenowski, O., Forster, C., Branscheid, D., Aufderheide, M., 2015. Int J. Environ. Res. Public Health 12 (4), 3915–3925.
Sussan, T.E., Gajghate, S., Thimmulappa, R.K., Ma, J.F., Kim, J.H., Sudini, K., Consolini, N., Cormier, S.A., Lomnicki, S., Hasan, F., Pekosz, A., Biswal, S., 2015. PLoS One 10, 2.
Williams, M., Talbot, P., 2011. Nicotine Tob. Res. 13 (12), 1276–1283.
Williams, M., Villarreal, A., Bozhilov, K., Lin, S., Talbot, P., 2013. PLoS One 8, 3.